

Electron parallel closures for various ion charge numbers

Journal-ref: Phys. Plasmas 23, 032124 (2016) **with corrections**

Jeong-Young Ji,^{1,*} Sang-Kyeun Kim,² Eric D. Held,¹ and Yong-Su Na²

¹*Department of Physics, Utah State University, Logan, Utah 84322*

²*Department of Nuclear Engineering,
Seoul National University, Seoul 151-742, Korea*

Abstract

Electron parallel closures for the ion charge number $Z = 1$ [J.-Y. Ji and E. D. Held, Phys. Plasmas **21**, 122116 (2014)] are extended for $1 \leq Z \leq 10$. Parameters are computed for various Z with the same form of the $Z = 1$ kernels adopted. The parameters are smoothly varying in Z and hence can be used to interpolate parameters and closures for noninteger, effective ion charge numbers.

*Electronic address: j.ji@usu.edu

I. INTRODUCTION

A set of fluid equations for density (n), temperature (T), and flow velocity (\mathbf{V}) require closure relations for heat flux density (\mathbf{h}), friction force density (\mathbf{R}), and viscous pressure tensor ($\boldsymbol{\pi}$). For electron-ion plasmas in a magnetic field, a complete set of closures has been obtained for high collisionality [1, 2]. In a magnetized plasma, parallel closures for moderate- and low-collisionality plasma are studied with approximate collision operators in Refs. [3–7]. Accurate collision operators [8, 9] are adopted in the general moment approach [8, 9]. In general, the parallel closures are expressed by kernel-weighted integrals. The kernels obtained from the moment method appear in a series of exponential functions and are valid up to moderately low collisionality depending on the number of moments. Closures in the collisionless limit have been studied in Refs. [3, 10–12].

From the moment kernels and collisionless kernels, simple fitted kernels for arbitrary collisionality are obtained for $Z = 1$ in Ref. [13]. For completeness and application to various ion charge numbers [14–16], we extend the $Z = 1$ work to $1 < Z \leq 10$. The fitted kernels are specified by seven parameters and the parameters have many local minima in the least square fitting. Among them we choose minima where parameters change smoothly in Z . The smoothness enables us to compute kernel parameters and closures for a noninteger effective ion charge number Z_{eff} .

In Sec. II, we review the parallel moment equations and the properties of kernels for the integral closures. In Sec. III, the fitted kernel parameters and accuracy of closures are presented for $1 \leq Z \leq 10$. In Sec. IV we summarize.

II. PARALLEL MOMENT EQUATIONS AND INTEGRAL CLOSURES

To obtain closures for the Maxwellian (M) moment equations, we decompose a distribution function into the Maxwellian (f^{M}) and non-Maxwellian parts (f^{N}), and then solve a reduced (approximate) kinetic equation for f^{N} . For *parallel* closures, we solve a drift kinetic equation to find a gyro-averaged distribution function (\bar{f}),

$$v_{\parallel} \frac{\partial f_e^{\text{N}}}{\partial \ell} = \overline{C_{\text{eL}}(f_e^{\text{N}})} - v_{\parallel} \frac{\partial \bar{f}_e^{\text{M}}}{\partial \ell} + \overline{C_{\text{eL}}(f_e^{\text{M}})} \quad (1)$$

for \bar{f}_e^{N} in terms of \bar{f}_e^{M} , where C_{eL} is the linearized Landau-Fokker-Planck operator with respect to $f_{a=e,i}^{\text{M}}$ for an electron distribution function F ,

$$C_{\text{eL}}(F) = C(F, f_e^{\text{M}}) + C(f_e^{\text{M}}, F) + C(F, f_i^{\text{M}}). \quad (2)$$

When solving Eq. (1) for closures, we must remove the fluid moment equations to be closed [12].

In the total-velocity moment expansion, the distribution functions are

$$f_a^M \approx f_a^m \left(1 + 2\mathbf{s}_a \cdot \frac{\mathbf{V}_a}{v_{Ta}}\right) = f_a^m + f_a^{M-m}, \quad (3)$$

$$f_a^N = f_a^m \sum_{lk \neq M} \hat{\mathbf{P}}_a^{lk} \cdot \mathbf{M}_a^{lk}, \quad (4)$$

with

$$f_a^m = n_a \hat{f}_a^m, \quad \hat{f}_a^m = \frac{1}{\pi^{3/2} v_{Ta}^3} e^{-s_a^2}, \quad (5)$$

and

$$\hat{\mathbf{P}}_a^{lk} = \frac{1}{\sqrt{\sigma_l \lambda_k^l}} \mathbf{P}_a^{lk}, \quad \mathbf{P}_a^{lk} = \mathbf{P}^l(\mathbf{s}_a) L_k^{(l+1/2)}(s_a^2). \quad (6)$$

Here $\mathbf{s}_a = \mathbf{v}/v_{Ta}$, $v_{Ta} = \sqrt{2T_a/m_a}$, \mathbf{V}_a is the flow velocity, $\sigma_l = l!/(2l+1)!!$, $\lambda_k^l = (l+k+1/2)!/k!(1/2)!$, \mathbf{P}^l is a harmonic tensor, and $L_k^{(l+1/2)}$ is a Laguerre-Sonine polynomial. Now the collision operators can be further linearized with respect to f_e^m and f_i^m ,

$$C_{eL}(f_e^N) \approx C(f_e^N, f_e^m) + C(f_e^m, f_e^N) + C(f_e^N, f_i^m), \quad (7)$$

and

$$C_{eL}(f_e^M) = C(f_e^M, f_i^m) \approx C(f_e^m, f_i^m) + C(f_e^{M-m}, f_i^m) + C(f_e^m, f_i^{M-m}). \quad (8)$$

The gyro-averaged distribution function, $\bar{f} = (2\pi)^{-1} \int d\gamma f$ where γ is the gyro-angle, can be written as

$$\bar{f}_a^M \approx \bar{f}_a^m \left(1 + 2s_{a\parallel} \frac{V_{a\parallel}}{v_{Ta}}\right) = \bar{f}_a^m + \bar{f}_e^{M-m}, \quad (9)$$

$$\bar{f}_a^N = \bar{f}_a^m \sum_{lk \neq M} \hat{\mathbf{P}}_a^{lk} n_a^{lk}, \quad (10)$$

with

$$\hat{\mathbf{P}}_a^{lk} = \frac{1}{\sqrt{\bar{\sigma}_l \lambda_k^l}} \mathbf{P}_a^{lk}, \quad \mathbf{P}_a^{lk} = s_a^l P_l(\xi) L_k^{(l+1/2)}(s_a^2), \quad (11)$$

$$n_a^{lk} = \sqrt{\frac{\bar{\sigma}_l}{\sigma_l}} n_a M_{a\parallel}^{lk}, \quad (12)$$

where $\bar{\sigma}_l = 1/(2l+1)$, $\xi = v_{\parallel}/v$, and P_l is a Legendre polynomial. It has been shown [17] that the gyroaverage of the linearized operators of distribution functions, Eqs. (7) and (8), are the same as the linearized operators of the gyroaveraged distribution functions, i.e.,

$$\overline{C_{eL}(f_e^N)} \approx C(\bar{f}_e^N, \bar{f}_e^m) + C(\bar{f}_e^m, \bar{f}_e^N) + C(\bar{f}_e^N, \bar{f}_i^m) \quad (13)$$

and

$$\overline{C_{eL}(f_e^M)} \approx C(f_e^m, f_i^m) + C(\bar{f}_e^{M-m}, f_i^m) + C(f_e^m, \bar{f}_i^{M-m}). \quad (14)$$

To obtain the (j, p) moment equation, we multiply \hat{P}^{jp} to Eq. (1) and integrate over velocity space

$$v_T \sum_{lk \neq M} \bar{\Psi}^{jp, lk} \frac{\partial n^{lk}}{\partial \ell} = \frac{1}{\tau_{ee}} \sum_{lk \neq M} c^{jp, lk} n^{lk} + \frac{1}{\tau_{ee}} g^{jp}, \quad (15)$$

where

$$\bar{\Psi}^{jp, lk} = \int d\mathbf{v} \hat{P}^{jp} s_{\parallel} \hat{f}^m \hat{P}^{lk}, \quad (16)$$

$$c^{jp, lk} = \tau_{ee} \int d\mathbf{v} \hat{P}^{jp} C_{eL}(\hat{f}^m \hat{P}^{lk}) = \delta_{jl} c_{pk}^j, \quad (17)$$

and

$$g^{jp} = \int d\mathbf{v} \hat{P}^{jp} [\tau_{ee} \overline{C_{eL}(f_e^M)} - \lambda_C s_{\parallel} \frac{\partial \bar{f}_e^M}{\partial \ell}], \quad (18)$$

where $\lambda_C = v_T \tau_{ee}$ and τ_{ee} is the electron-electron collision time. The electron collision matrix can be computed from

$$c_{pk}^j = \frac{\tau_{ee}}{n_e \sqrt{\lambda_p^j \lambda_k^j}} (A_{ee}^{jpk} + B_{ee}^{jpk} + A_{ei}^{jpk}) \quad (19)$$

where

$$\bar{\sigma}_j A_{ab}^{jpk} = \int d\mathbf{v} P_a^{jp} C(f_a^m P_a^{jk}, f_b^m), \quad (20)$$

$$\bar{\sigma}_j B_{ab}^{jpk} = \int d\mathbf{v} P_a^{jp} C(f_a^m, f_b^m P_a^{jk}). \quad (21)$$

and formulae for A_{ab}^{jpk} and B_{ab}^{jpk} are presented in Refs. [17, 18]. For electrons, the nonvanishing thermodynamic drives g_A are

$$g^{1k} = \delta_{1k} \frac{\sqrt{5}}{2} \frac{n}{T} \frac{dT}{d\eta} + \sqrt{2} Z a_{ei}^{1k0} n \hat{V}_{ei\parallel}, \quad (22)$$

$$g^{20} = -\frac{\sqrt{3}}{2} n \tau_{ee} W_{\parallel}, \quad (23)$$

where

$$a_{ei}^{10k} = a_{ei}^{1k0} = -\sqrt{\frac{3(k+1/2)!}{(2k+3)k!(1/2)!}}, \quad (24)$$

$$\hat{V}_{ei\parallel} = \frac{\mathbf{b} \cdot (\mathbf{V}_e - \mathbf{V}_i)}{v_T}, \quad (25)$$

and

$$W_{\parallel} = \mathbf{b} \mathbf{b} : \mathbf{W}, \quad (\mathbf{W})_{\alpha\beta} = \partial_{\alpha} V_{\beta} + \partial_{\beta} V_{\alpha} - \frac{2}{3} \delta_{\alpha\beta} \nabla \cdot \mathbf{V}. \quad (26)$$

The parallel closures are related to the general moments by

$$h_{\parallel} = -\frac{\sqrt{5}}{2}v_T T n^{11}, \quad (27)$$

$$R_{\parallel} = \frac{m_e v_{Te}}{\tau_{ei}} [-n_e \hat{V}_{ei\parallel} + \frac{1}{\sqrt{2}} \sum_{k=1} a_{ei}^{10k} n^{1k}], \quad (28)$$

$$\pi_{\parallel} = \frac{2}{\sqrt{3}} T n^{20}. \quad (29)$$

When solving Eq. (15), we truncate the system with $j, l = 0, 1, \dots, L-1$ and

$$p, k = \begin{cases} 2, 3, \dots, K+1, & l = 0 \\ 1, 2, \dots, K, & l = 1 \\ 0, 1, \dots, K-1, & l = 2, \dots, L-1 \end{cases}$$

to have a system of $N = LK$ moment equations. Enumerating the moment indices (l, k) as a single index $A = lK + k + \iota = 1, 2, \dots, N$, where

$$\iota = \begin{cases} -1, & l = 0 \\ 0, & l = 1 \\ +1, & l = 2, \dots, L-1 \end{cases}$$

we rewrite Eq. (15) as

$$\sum_{B=1}^N \Psi_{AB} \frac{\partial n_B}{\partial \eta} = \sum_{B=1}^N C_{AB} n_B + g_A. \quad (30)$$

Here the arlength ℓ along a magnetic field line is normalized by the collision length, $d\eta = d\ell/\lambda_C$. The linear system (30) with constant matrices Ψ and C can be solved by computing the eigensystem of $\Psi^{-1}C$ (see Refs. [8] and [9] for details):

$$\sum_C (\Psi^{-1}C)_{AB} W_{BC} = k_D W_{AC}, \quad (31)$$

where the eigenvalues k_D appear in positive and negative pairs. The particular solution driven by thermodynamic drives is

$$n_A(z) = \sum_D \int_{-\infty}^{\infty} K_{AD}(z-z') g_D(z') dz', \quad (32)$$

where the kernel functions are defined by

$$K_{AD}(\eta) = \begin{cases} - \sum_{\{B|k_B>0\}}^N \gamma_{AD}^B e^{k_B \eta}, & \eta < 0, \\ + \sum_{\{B|k_B<0\}}^N \gamma_{AD}^B e^{k_B \eta}, & \eta > 0, \end{cases} \quad (33)$$

with coefficients

$$\gamma_{AD}^B = \sum_C W_{AB} W_{BC}^{-1} \Psi_{CD}^{-1}. \quad (34)$$

For closure moments, we define

$$\begin{aligned} \gamma_{hh}^B &= \frac{5}{2} \gamma_{11,11}^B, \\ \gamma_{hR}^B &= -\sqrt{\frac{5}{2}} \sum_{k=1}^M a_{ei}^{1k0} \gamma_{11,1k}^B = \gamma_{Rh}^B, \\ \gamma_{h\pi}^B &= -\sqrt{\frac{5}{3}} \gamma_{11,20}^B = \gamma_{\pi h}^B, \\ \gamma_{RR}^B &= \sum_{p,k=1}^M a_{ei}^{10p} a_{ei}^{1k0} \gamma_{1p,1k}^B, \\ \gamma_{R\pi}^B &= +\sqrt{\frac{2}{3}} \sum_{k=1}^M a_{ei}^{1k0} \gamma_{20,1k}^B = \gamma_{\pi R}^B, \\ \gamma_{\pi\pi}^B &= \frac{4}{3} \gamma_{20,20}^B, \end{aligned} \quad (35)$$

and corresponding K_{AD} by Eq. (33). Noting that

$$\gamma_{AD}^{-B} = \begin{cases} -\gamma_{AD}^B, & AD = hh, hR, RR, \pi\pi \equiv \text{even}, \\ +\gamma_{AD}^B, & AD = h\pi, R\pi \equiv \text{odd}, \end{cases} \quad (36)$$

where $-B$ denotes the moment index corresponding to $-k_B$, we notice that the kernel functions are even or odd functions:

$$K_{AD}(-\eta) = \begin{cases} +K_{AD}(\eta), & AD = \text{even} \\ -K_{AD}(\eta), & AD = \text{odd}. \end{cases} \quad (37)$$

Using the definition of K_{AD} and Eqs. (22)-(29), we can write the parallel closures as

$$h_{\parallel}(\ell) = T v_T \int d\eta' \left(-\frac{1}{2} K_{hh} \frac{n}{T} \frac{dT}{d\eta'} + K_{hR} Z n \frac{V_{ei\parallel}}{v_T} - K_{h\pi} \frac{3}{4} n \tau_{ee} W_{\parallel} \right), \quad (38)$$

$$R_{\parallel}(\ell) = -\frac{mn}{\tau_{ei}} V_{ei\parallel} + \frac{m v_T}{\tau_{ei}} \int d\eta' \left(-K_{Rh} \frac{n}{2T} \frac{dT}{d\eta'} + K_{RR} Z n \frac{V_{ei\parallel}}{v_T} - K_{R\pi} \frac{3}{4} n \tau_{ee} W_{\parallel} \right), \quad (39)$$

$$\pi_{\parallel}(\ell) = T \int d\eta' \left(-K_{\pi h} \frac{n}{T} \frac{dT}{d\eta'} + 2K_{\pi R} Z n \frac{V_{ei\parallel}}{v_T} - K_{\pi\pi} \frac{3}{4} n \tau_{ee} W_{\parallel} \right). \quad (40)$$

The closure calculation from a truncated moment system involves truncation errors which depend on the collisionality. The inverse collisionality is often measured by the Knudsen number

$k = \lambda_C/|\nabla^{-1}|$. Since the sinusoidal drives have a constant k , we use them to investigate the truncation errors and convergent behavior of the closures while increasing the number of moments N . Furthermore, in many practical applications, general drives can be expressed by Fourier series in a periodic system or its continuum version, Fourier transform, in a non-periodic system.

For sinusoidal drives, $T = T_0 + T_1 \sin \varphi$, $V_{\parallel} = V_0 + V_1 \sin \varphi$, and $V_{\text{ei}\parallel} = V_{\text{ei}} \cos \varphi$, where $\varphi = 2\pi\ell/\lambda + \varphi_0 = k\eta + \varphi_0$ and $k = 2\pi\lambda_C/\lambda$, assuming that n and $v_T \approx \sqrt{2T_0/m}$ are constant and $\nabla \cdot \mathbf{V}_{\perp} \approx 0$, the linearized closures become

$$h_{\parallel}(\ell) = -\frac{1}{2}nT_1v_T\hat{h}_h \cos \varphi + nT_0V_{\text{ei}}\hat{h}_R \cos \varphi - nT_0V_1\hat{h}_{\pi} \sin \varphi, \quad (41)$$

$$R_{\parallel}(\ell) = -nT_1\frac{2\pi}{\lambda}\hat{R}_h \cos \varphi - \frac{mnV_{\text{ei}}}{\tau_{\text{ei}}}\hat{R}_R \cos \varphi - nmV_1\frac{2\pi v_T}{\lambda}\hat{R}_{\pi} \sin \varphi, \quad (42)$$

$$\pi_{\parallel}(\ell) = -nT_1\hat{\pi}_h \sin \varphi + 2nT_0\frac{V_{\text{ei}}}{v_T}\hat{\pi}_R \sin \varphi - nT_0\frac{V_1}{v_T}\hat{\pi}_{\pi} \cos \varphi. \quad (43)$$

The dimensionless closures are defined by $\hat{h}_h = k\hat{K}_{hh}$, $\hat{h}_R = Z\hat{K}_{hR} = \hat{R}_h$, $\hat{h}_{\pi} = k\hat{K}_{h\pi} = \hat{\pi}_h$, $\hat{R}_R = 1 - Z\hat{K}_{RR}$, $\hat{R}_{\pi} = Z\hat{K}_{R\pi} = \hat{\pi}_R$, and $\hat{\pi}_{\pi} = k\hat{K}_{\pi\pi}$, where

$$\hat{K}_{AD} = \begin{cases} \sum_{B=1}^N \frac{-\gamma_{AD}^B k_B}{k_B^2 + k^2}, & AD = \text{even} \\ \sum_{B=1}^N \frac{\gamma_{AD}^B k}{k_B^2 + k^2}, & AD = \text{odd}, \end{cases} \quad (44)$$

which are derived from Eq. (33), Eq. (36), and

$$\int K_{AD}(\eta - \eta') \cos(k\eta' + \varphi_0) d\eta' = \begin{cases} \hat{K}_{AD} \cos \varphi, & AD = \text{even}, \\ \hat{K}_{AD} \sin \varphi, & AD = \text{odd}. \end{cases} \quad (45)$$

III. FITTED KERNEL FUNCTIONS FOR INTEGRAL CLOSURES

The kernel functions obtained from N moment equations, Eq. (33), (i) consist of $N/2$ terms of exponential functions, and (ii) are inaccurate for $\eta \lesssim \eta_c$ where η_c decreases as N increases (e.g. $\eta_c \sim 0.01$ for $N = 6400$). The inaccuracy for small η introduces an error in the closure calculation for large wave number $k \gtrsim k_c$. For example, in the case of the parallel heat flow with $Z = 1$ (see Fig. 2 of Ref. [13]), the $N = 100$ result deviates less than 1% from the $N = 400$ result for $k \lesssim 5$. This means that the $N = 400$ result is accurate within much less than 1% error for $k \lesssim 5$. Similarly, the $N = 400$ result agrees with the $N = 1600$ result for $k \lesssim 20$ and the $N = 1600$ result agrees with the $N = 6400$ result for $k \lesssim 80$. As a conservative estimate, $k_c \sim 80$ and the

$N = 6400$ heat flow closure is practically exact for $k \lesssim k_c$. This convergence scheme can be used to estimate how many parallel moments are needed for a given k value. To be accurate within 1% error, $N = 100$ is required for $k \sim 5$, $N = 400$ for $k \sim 20$, $N = 1600$ for $k \sim 80$, and so on. Note that the $N = 6400$ kernels consist of 3200 terms and are accurate only for $k \lesssim 80$. Therefore, it is desirable to obtain simple fitted functions that accurately represent the moment-solution kernels for $\eta \gtrsim \eta_c$, and the collisionless kernels for $\eta \lesssim \eta_c$. We obtained the fitted kernels for $Z = 1$ in Ref. [13] and extend to $Z = 2, 3, \dots, 10$ in this work.

In the collisional limit, the parallel closures for arbitrary Z are [19]

$$h_{\parallel} = -\hat{\kappa}_{\parallel} \frac{nT\tau_{ee}}{m} \partial_{\parallel} T + \hat{\beta}_{\parallel} nTV_{ei\parallel}, \quad (46)$$

$$R_{\parallel} = -\hat{\beta}_{\parallel} n \partial_{\parallel} T - \hat{\alpha}_{\parallel} \frac{mn}{\tau_{ei}} V_{ei\parallel}, \quad (47)$$

$$\pi_{\parallel} = -\hat{\eta}_0 nT\tau_{ee} W_{\parallel}. \quad (48)$$

In the collisionless limit, the closures are determined from the asymptotic behavior of the kernels for $\eta \ll 1$

$$K_{hh}(\eta) \approx -\frac{18}{5\pi^{3/2}} (\ln |\eta| + \gamma_h), \quad (49)$$

$$K_{h\pi}(\eta) \approx \frac{1}{5}, \quad (50)$$

$$K_{\pi\pi}(\eta) \approx -\frac{4}{5\pi^{1/2}} (\ln |\eta| + \gamma_{\pi}), \quad (51)$$

where γ_h and γ_{π} are constants [12]. For the friction related kernels K_{hR} , K_{RR} , and $K_{R\pi}$, extrapolating the 6400 moment solution with the constraint Eq. (46) will be accurate enough since the corresponding closures vanish as $\tau \rightarrow \infty$ ($k \rightarrow \infty$, in the collisionless limit).

All kernel functions are fitted to a single function with the same form of $Z = 1$ kernels adopted,

$$K_{AB}(\eta) = -[d + a \exp(-b\eta^c)] \ln[1 - \alpha \exp(-\beta\eta^{\gamma})]. \quad (52)$$

The parameters a , b , c , d , α , β , and γ are listed in Table I.

In computing the fitted kernel parameters there are many least-squares local minima which accurately represent the convergent kernels ($\eta \gtrsim 0.01$). We use sinusoidal drives to assess the accuracy of fitted kernels. The closures computed from fitted kernels are compared with 6400 moment closures in the convergent regime ($k \lesssim 80$). Note that the fitted parameters automatically satisfy kernels for $\eta \lesssim 0.01$ forced by Eqs. (49)-(51) and therefore closures for K_{hh} , $K_{h\pi}$, and $K_{\pi\pi}$ are accurate in the collisionless limit. For friction related kernels K_{hR} , $K_{R\pi}$, and K_{RR} , the closures are ignorable in the collisionless (no friction) limit.

K_{AB}	Z	1	2	3	4	5	6	7	8	9	10
K_{hh}	a	-3.85	-3.61	-4.02	-4.50	-5.52	-6.98	-9.59	-14.8	-24.2	-39.0
	b	0.248	0.387	0.590	0.746	0.796	0.776	0.686	0.528	0.377	0.267
	c	0.680	0.551	0.537	0.569	0.581	0.583	0.583	0.583	0.583	0.583
	d	5.40	5.47	6.07	6.66	7.74	9.28	11.9	17.1	26.5	41.4
	α	1	1	1	1	1	1	1	1	1	1
	β	2.02	2.49	2.91	3.20	3.46	3.70	3.93	4.18	4.43	4.65
	γ	0.417	0.348	0.316	0.300	0.291	0.281	0.279	0.277	0.276	0.275
K_{hR}	a	6.37	6.76	5.63	5.34	5.61	6.31	8.22	11.3	17.3	27.9
	b	5.12	5.72	6.09	6.53	6.85	7.06	7.31	7.51	7.61	7.71
	c	0.160	0.179	0.219	0.240	0.239	0.227	0.205	0.181	0.154	0.126
	d	0.100	0.187	0.339	0.440	0.465	0.457	0.411	0.374	0.325	0.278
	α	1	1	1	1	1	1	1	1	1	1
	β	1.00	1.73	2.50	2.96	3.19	3.33	3.37	3.39	3.37	3.34
	γ	0.583	0.465	0.387	0.346	0.332	0.326	0.327	0.327	0.328	0.329
$K_{h\pi}$	a	-0.229	-0.179	-0.144	-0.133	-0.130	-0.137	-0.150	-0.169	-0.212	-0.239
	b	2.26	3.08	3.72	4.35	4.72	4.94	5.05	5.12	5.15	5.38
	c	0.594	0.596	0.594	0.588	0.569	0.562	0.556	0.551	0.548	0.543
	d	0.363	0.280	0.240	0.225	0.210	0.220	0.241	0.269	0.308	0.334
	α	0.775	0.862	0.875	0.886	0.918	0.910	0.889	0.865	0.875	0.878
	β	1.49	1.69	1.81	1.97	2.12	2.32	2.53	2.76	3.03	3.23
	γ	0.478	0.460	0.454	0.442	0.432	0.415	0.399	0.380	0.362	0.351
K_{RR}	a	305	322	342	363	386	406	431	450	470	489
	b	8.30	8.67	8.90	9.09	9.23	9.32	9.40	9.49	9.52	9.54
	c	0.139	0.140	0.141	0.142	0.143	0.143	0.144	0.144	0.144	0.144
	d	0.362	0.459	0.576	0.686	0.830	0.972	1.14	1.30	1.47	1.67
	α	1	1	1	1	1	1	1	1	1	1
	β	3.24	4.11	4.75	5.23	5.68	6.06	6.39	6.71	6.97	7.24
	γ	0.349	0.314	0.290	0.272	0.258	0.248	0.237	0.232	0.225	0.219
$K_{R\pi}$	a	0.102	0.125	0.147	0.169	0.186	0.209	0.224	0.239	0.253	0.263
	b	0.528	0.724	0.898	1.06	1.22	1.30	1.51	1.61	1.77	1.91
	c	0.961	0.948	0.922	0.901	0.887	0.864	0.848	0.832	0.823	0.818
	d	0.198	0.212	0.225	0.230	0.231	0.225	0.220	0.213	0.207	0.202
	α	1	1	1	1	1	1	1	1	1	1
	β	2.45	3.06	3.52	3.87	4.15	4.38	4.57	4.73	4.88	5.02
	γ	0.408	0.370	0.347	0.332	0.322	0.313	0.307	0.303	0.299	0.294
$K_{\pi\pi}$	a	0.470	0.598	0.700	0.762	0.804	0.839	0.857	0.873	0.878	0.883
	b	1.06	1.19	1.31	1.45	1.59	1.72	1.85	1.97	2.08	2.18
	c	0.661	0.607	0.580	0.566	0.557	0.551	0.546	0.543	0.541	0.539
	d	0.357	0.275	0.207	0.166	0.139	0.118	0.106	0.096	0.091	0.087
	α	1	1	1	1	1	1	1	1	1	1
	β	1.66	1.97	2.17	2.34	2.49	2.61	2.74	2.85	2.97	3.08
	γ	0.546	0.517	0.498	0.487	0.479	0.472	0.469	0.466	0.465	0.465

Table I: Fitted parameters in Eq. (52) for $Z = 1, 2, \dots, 10$.

In the interest of including noninteger effective ion charge numbers, we choose sets of least-squares fitting parameters that change smoothly in Z . Although some parameters for $Z = 1$ in this work are different from the ones in Ref. [13], they provide similar accuracy for closure calculations. For a noninteger ion-charge number Z_{eff} , $Z < Z_{\text{eff}} < Z + 1$, a simple linear interpolation of parameters $A = a, b, c, d, \beta, \gamma$

$$A_{Z_{\text{eff}}} = (1 + Z - Z_{\text{eff}})A_Z + (Z_{\text{eff}} - Z)A_{Z+1} \quad (53)$$

results in accurate results. We note that using the constraints (49)-(51) instead of interpolating all parameters results in higher accuracy. We obtain a from other interpolated parameters for K_{hh} and $K_{\pi\pi}$

$$a = \frac{18}{5\pi^{3/2}\gamma} - d \text{ for } K_{hh}, \quad (54)$$

$$a = \frac{4}{5\pi^{1/2}\gamma} - d \text{ for } K_{\pi\pi}, \quad (55)$$

and α for $K_{h\pi}$

$$\alpha = 1 - \exp \frac{-1}{5(a+d)} \text{ for } K_{h\pi}. \quad (56)$$

The maximum deviations from the closures in the convergent regime ($k \lesssim 80$) are shown for integers and half-integers in Table II. The maximum deviations usually occur at k where the closure values are close to zero. For a noninteger $Z < Z_{\text{eff}} < Z + 1$, the error is less than the maximum of errors at Z , $Z + 1/2$, and $Z + 1$. The maximum errors are less than 5% at the worst case for any arbitrary $1 \leq Z \leq 10$.

Fig. 1 shows typical behavior of closures due to sinusoidal drives for various Z . In the collisional ($k \ll 1$) limit, the closures approach the corresponding high-collisionality values for each Z [19]. In the collisionless ($k \rightarrow \infty$) limit, the closures approach Z -independent collisionless-limit values [12]. Although the maximum errors are verified to be less than 5% for $k \lesssim 80$, the errors may be larger than 5% for $k \gtrsim 80$. Since the exact values are unknown in this regime (the 6400 moment closures do not converge) we can only estimate the accuracy of closures from the shape of curves. In this regime, the change of closure values \hat{h}_h for $Z = 10$ and $h_{\hat{\pi}}$ ($\hat{\pi}_h$) for $Z = 5, 10$ seems slightly eccentric. Nevertheless, the errors are expected to be not much greater than 5%, since the closure values eventually approach the theoretical values in the collisionless limit.

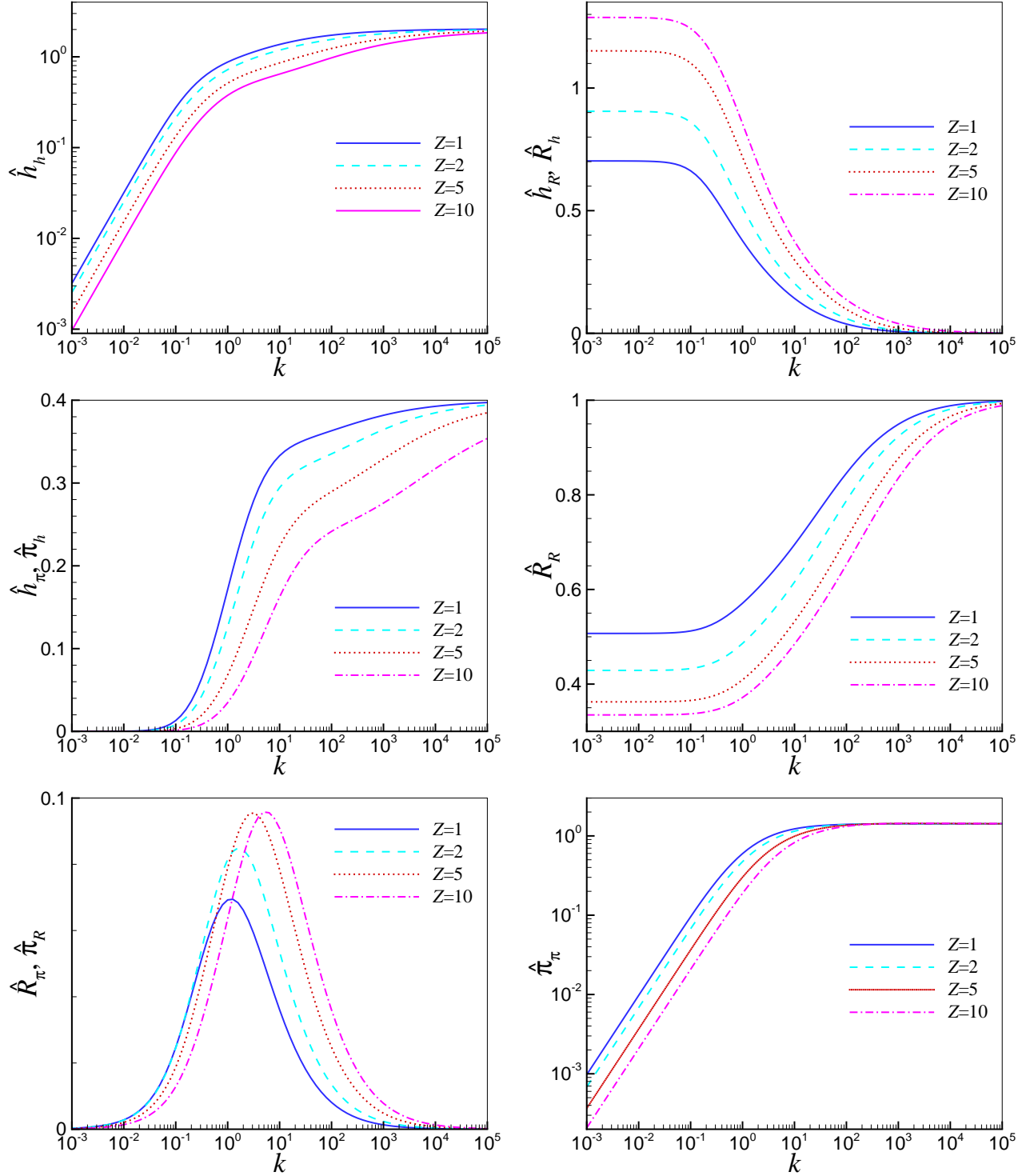


Figure 1: (Color online) Closures for sinusoidal drives computed from fitted kernels for $Z = 1, 2, 5,$ and 10 .

Z	\hat{K}_{hh}	\hat{K}_{hR}	$\hat{K}_{h\pi}$	\hat{K}_{RR}	$\hat{K}_{R\pi}$	$\hat{K}_{\pi\pi}$
1	1.0	0.6	0.6	0.7	1.0	0.5
1.5	2.4	3.2	2.7	4.0	3.2	1.6
2	2.8	0.9	1.0	0.7	0.9	0.8
2.5	3.0	4.4	1.8	2.4	1.5	1.1
3	4.9	1.9	0.7	0.7	0.6	0.6
3.5	4.3	2.3	1.1	1.5	0.9	1.0
4	4.8	4.3	0.8	0.3	0.3	0.4
4.5	4.4	4.1	1.2	0.8	0.9	0.5
5	4.7	4.4	0.8	0.2	0.5	0.4
5.5	4.2	3.7	0.8	0.3	0.8	0.4
6	4.6	3.9	0.8	0.5	0.5	0.4
6.5	3.1	1.0	0.8	0.3	0.6	0.2
7	3.1	0.8	1.0	0.4	0.7	0.5
7.5	2.8	1.5	1.4	0.2	0.5	0.4
8	3.0	0.9	2.0	0.2	0.7	0.4
8.5	3.7	4.0	2.3	0.3	0.9	0.4
9	3.4	1.8	2.5	0.2	0.9	0.5
9.5	3.4	3.1	2.6	0.3	0.7	0.3
10	3.4	3.2	2.7	0.8	0.9	0.3

Table II: Maximum percentage deviation of closures computed with fitted kernels from 6400 moment closures in the convergent regime $\eta \lesssim 80$ for $1 \leq Z \leq 10$. For half integers, kernel parameters are computed by linear interpolation.

IV. SUMMARY

In obtaining simple fitted kernels for electron parallel closures, we extended the $Z = 1$ calculation to $Z = 2, \dots, 10$. Since parameters change smoothly in Z , linear interpolation of parameters at Z and $Z + 1$ yields the parameter for noninteger $Z < Z_{\text{eff}} < Z + 1$ with the same order of accuracy in computing closures.

The same method can be applied to ion parallel closures. As shown in Refs. [9, 20], inclusion of the ion-electron collision operator is necessary. The ion-electron operator introduces two independent parameters, the mass ratio combined with the ion charge number and the temperature ratio. Fitted kernels for ion parallel closures will appear in future work.

Acknowledgments

One of the authors (Ji) would like to thank the Fusion and Plasma Application Laboratory (FUSMA) Team at Seoul National University for their kind support during his visit. The research was supported by the U.S. DOE under grant nos. de-sc0014033, DE-FG02-04ER54746, DE-FC02-04ER54798, and DE-FC02-05ER54812, and by the National R&D Program through the National Research Foundation of Korea (NRF), funded by the Ministry of Science, ICT & Future Planning (No. 2014-M1A7A1A03045368), and by the project PE15090 of Korea Polar Research Institute. This work was performed in conjunction with the Plasma Science and Innovation (PSI) Center and the Center for Extended MHD Modeling (CEMM).

- [1] S. I. Braginskii, *Sov. Phys. JETP* **6**, 358 (1958).
- [2] S. I. Braginskii, in *Reviews of Plasma Physics*, edited by M. A. Leontovich (Consultants Bureau, New York, 1965), vol. 1, p. 205.
- [3] Z. Chang and J. D. Callen, *Phys. Fluids B* **4**, 1167 (1992).
- [4] E. D. Held, J. D. Callen, C. C. Hegna, and C. R. Sovinec, *Phys. Plasmas* **8**, 1171 (2001).
- [5] E. D. Held, *Phys. Plasmas* **10**, 4708 (2003).
- [6] E. D. Held, J. D. Callen, and C. C. Hegna, *Phys. Plasmas* **10**, 3933 (2003).
- [7] E. D. Held, J. D. Callen, C. C. Hegna, C. R. Sovinec, T. A. Gianakon, and S. E. Kruger, *Phys. Plasmas* **11**, 2419 (2004).
- [8] J.-Y. Ji, E. D. Held, and C. R. Sovinec, *Phys. Plasmas* **16**, 022312 (2009).
- [9] J.-Y. Ji and E. D. Held, *J. Fusion Energy* **28**, 170 (2009).
- [10] G. W. Hammett and F. W. Perkins, *Phys. Rev. Lett.* **64**, 3019 (1990).
- [11] R. D. Hazeltine, *Phys. Plasmas* **5**, 3282 (1998).
- [12] J.-Y. Ji, E. D. Held, and H. Jhang, *Phys. Plasmas* **20**, 082121 (2013).
- [13] J.-Y. Ji and E. D. Held, *Phys. Plasmas* **21**, 122116 (2014).
- [14] G. Lee, J. Kim, S. Hwang, C. Chang, H. Chang, M. Cho, B. Choi, K. Kim, K. Cho, S. Cho, et al., *Nuclear Fusion* **40**, 575 (2000).
- [15] S. K. Rathgeber, R. Fischer, S. Fietz, J. Hobirk, A. Kallenbach, H. Meister, T. Pütterich, F. Ryter, G. Tardini, E. Wolfrum, et al., *Plasma Physics and Controlled Fusion* **52**, 095008 (2010).

- [16] A. Kallenbach, M. Bernert, R. Dux, L. Casali, T. Eich, L. Giannone, A. Herrmann, R. McDermott, A. Mlynek, H. W. Müller, et al., *Plasma Physics and Controlled Fusion* **55**, 124041 (2013).
- [17] J.-Y. Ji and E. D. Held, *Phys. Plasmas* **13**, 102103 (2006).
- [18] J.-Y. Ji and E. D. Held, *Phys. Plasmas* **15**, 102101 (2008).
- [19] J.-Y. Ji and E. D. Held, *Phys. Plasmas* **20**, 042114 (2013).
- [20] J.-Y. Ji and E. D. Held, *Phys. Plasmas* **22**, 062114 (2015).